Dalton Transactions

ROYAL SOCIETY OF CHEMISTRY

PAPER

View Article Online
View Journal

Cite this: DOI: 10.1039/d6dt00207b

Structural design principles for hybrid cadmium thiocyanate-halides containing bulky organic cations

Alexander Milder and Patrick M. Woodward *

Received 26th January 2026,
Accepted 20th March 2026

DOI: 10.1039/d6dt00207b

rsc.li/dalton

Seven new hybrid cadmium thiocyanate-halide compounds are reported that feature protonated primary amines that are either branched (isopropylammonium, isobutylammonium), cyclic (cyclopentylammonium), or aromatic (benzylammonium, anilinium). All seven compounds adopt structures that have one-dimensional (1D) chains or ribbons of Cd-centered octahedra linked through bridging thiocyanate groups. The nitrogen end of the thiocyanate linker coordinates to one Cd^{2+} ion in all cases, while the sulfur end coordinates to either one or two Cd^{2+} ions. As the size and/or bulkiness of the organic cation increases, the width of the inorganic chain/ribbon increases and the ratio of amine halide salt to $Cd(SCN)_2$ decreases. In all compounds, the halide ions are bound to only one Cd^{2+} ion, which allows them to act as a molecular scissor to break up the connectivity of the octahedral framework. The bandgaps of these compounds lie between 4.3 and 4.6 eV, with small variations depending mainly on the identity of the halide ion. The relatively narrow valence and conduction bands result from the inability of the bridging thiocyanate groups to facilitate strong electronic coupling between metal centers. However, the relatively large band gap of the inorganic framework may be attractive for incorporating optically active organic cations.

Introduction

Solid-state hybrid materials, combining organic and inorganic components cover an incredible range of structure types, elemental compositions, and ultimately, physical and chemical properties.[1–5] The ability of hybrid materials to form flexible and tunable compositions make them well suited to a variety of different applications.[2,6–9] Thiocyanate (SCN^-) linked hybrid materials have been shown to adopt a wide range of different structure types and play host to a variety of different cations.[10–15] Thiocyanates have been explored as electronic and phase change materials, as well as a platform for symmetry breaking effects.[6,16–19] However, the structural variability of hybrid thiocyanates make it difficult to rationally target new materials, as the key structure directing effects are complex and not well understood. By limiting the synthesis space to simple combination reactions between $Cd(SCN)_2$ and amine halide salts, a series of new thiocyanate materials have been prepared and characterized. The goal of this work is to understand how the size, shape, and conformational flexibility of the organic cation influences the structure and dimensionality of the inorganic framework. By maintaining the cadmium thiocyanate backbone and similar synthetic conditions it is possible to tease out the underlying structure-directing influences of the organic cation.

The crystal structures of the halide bridged layered perovskites, $Cs_2Pb(SCN)_2I_2$ and $(CH_3NH_3)_2Sn(SCN)_2Cl_2$, as well as the one dimensional thiocyanate bridged compounds $A_2Cd(SCN)_2Cl_2$ ($A = CH_3(CH_2)_nNH_3^+$, n = 0–3), demonstrate the importance of hydrogen bonding and the preferential binding mode of the thiocyanate anion as key structure directing influences.[19–23] Yet these compounds all contain relatively small, flexible organic cations, raising the question of how these structures respond to the incorporation of larger cations. Halide free thiocyanates containing either cadmium or copper and large, bulky amines, such as tetraethylethylenediamine and bipiperidine have been reported.[14,24–26] The 1D chains and ribbons of cadmium octahedra or the 2D and 3D constructs of copper tetrahedra are sufficiently flexible to accommodate large luminescent organic cations and charge-transfer supramolecular assemblies. Additionally, Xu *et al.* synthesized a number of mixed anion materials containing bulky organic cations and different ratios of thiocyanate and other anions and studied how the characteristics of the organic cation and/or small modifications to synthetic conditions affect anion incorporation.[14,24]

Building on previous studies, seven new hybrid thiocyanate-halide compounds were synthesized *via* simple combination reactions between amine halide salts and $Cd(SCN)_2$. By keeping the ions that make up the inorganic network the same

Department of Chemistry and Biochemistry, The Ohio State University, Columbus, Ohio 43210, USA. E-mail: woodward.55@osu.edu

from one compound to the next we aim to better understand the structure directing forces of the organic cations. The use of different protonated primary amines—cyclopentylammonium (CPA), isobutylammonium (IBA), isopentylammonium (IPA), benzylammonium (BzA), and anilinium (Ani) (Fig. S1)—results in different organizations of the inorganic framework and thus different stoichiometries. The structures of these compounds reveal secondary structure directing influences related to the packing of organic cations and how they countervail or act synergistically with preferred modes of hydrogen bonding. The insights obtained move us closer to the rational design of hybrid thiocyanate-halides with controlled inorganic substructures.

Experimental

All chemicals were used as received from the supplier without further purification. Amine salts were made by neutralization of the concentrated liquid amine (aniline: Mallinckrodt, 99%; cyclopentylamine: Fisher, 99%; isobutylamine: Acros Organics, 99%; isopentylamine: Alfa Aesar, 99%; benzylamine: Acros, >98%) with HCl (Fisher, 38%). After neutralization the resulting solution was evaporated to dryness and the salt was recrystallized from ethanol (Fisher, 95%) and washed with diethyl ether (Fisher, anhydrous). $Cd(SCN)_2$ was synthesized by mixing $Cd(NO_3)_2{\cdot}4H_2O$ (Mallinckrodt, 96%) and KSCN (Baker, 98%), each dissolved separately in methanol, for 30 minutes. The suspension was chilled in an ice bath, filtered to remove the solid KNO_3, and then evaporated to dryness *in vacuo* to produce $Cd(SCN)_2$. Compounds **1–7** were synthesized by combining 1 mmol of the appropriate amine halide salt with a stoichiometric amount of $Cd(SCN)_2$ in 12 mL of methanol (Fisher, >99.8%), stirring for 30 minutes, and then allowing the resultant solution to slowly evaporate. After 4–14 days, clear, needle, or bladed crystals were harvested and used either as is or ground to a powder for further analysis.

Single crystal X-ray diffraction (SCXRD) data were collected on a Bruker D8 Venture Diffractometer utilizing a high-intensity Mo (λ = 0.71073 Å) rotating anode source and a Photon III detector. Crystals were mounted on MiTeGen MicroMounts and encapsulated in clear laquer. Temperatures during measurement were measured at 298 or 100 K and controlled using an Oxford Cryosystems Cryostream. Collected data were integrated using the Bruker SAINT program and scaled and corrected for absorption using Bruker SADABS-2016/2.[27,28] Structures were solved using SHELXT 2018/2 and refined using SHELXL 2019/1 implemented in Olex2 1.5.[29,30] Ground single crystals were assessed for phase purity by powder X-ray diffraction (PXRD) using either a Bruker D8 Advance or Rigaku Miniflex II powder diffractometer.

UV-visible DRS data were collected on the ground single crystal samples from 225 nm to 800 nm with a PerkinElmer Lambda 950 spectrometer equipped with a 60 mm InGaAs integration sphere. Dry $BaSO_4$ (Alfa-Aesar, 97%) was used as the 100% reflectance standard and the data were transformed to pseudo-absorbance data using the Kubelka–Munk function.

Density functional theory (DFT) was used to calculate the electronic band structure and partial density of states (DOS) as implemented with Quantum ESPRESSO (ver. 6.1) in combination with the BURAI (ver. 1.3.1) GUI.[31,32]

Results

Crystal structures

The crystal structures of the seven compounds presented herein were solved from SCXRD data and share some general characteristics while differing slightly due to the packing of the organic cations and interactions with the halide anions. All seven compounds contain cadmium-centered octahedra with different ratios of terminal halide and bridging thiocyanate ligands. The number and bridging nature of the thiocyanate group, μ_2 or μ_3, determines if these octahedra form chains or ribbons of different sizes, which correspond to the different stoichiometries and symmetries of these compounds. Within isostructural sets of compounds more subtle changes to the structures are observed due to the size and shape of the cation and halide present in each material.

Compounds **1–4** are isostructural. They crystallize with $P\bar{1}$ space group symmetry and $ACd(SCN)_2X$ stoichiometry. All four compounds have a similar hydrogen bonding pattern that changes slightly depending on the identity of the halide ion and packing of the hydrocarbon tails of the organic cations. The structures of these clear needle and bladed crystals were solved using SCXRD either at 100 K or at room temperature. The details are given in Tables 1 and 2 with further information about the refinements in Table S1. The inorganic part of these compounds is characterized by one-dimensional (1D) ribbons of cadmium thiocyanate octahedra bridged by SCN^- ligands in a pseudo-edge sharing configuration. Each Cd is coordinated by three *mer* sulfur, two *trans* nitrogen, and one terminal halide ion within each octahedron. However, the feature that sets these compounds apart from some similar cadmium thiocyanate halides is that two of the SCN^- ligands are μ_3-bridging, such that these octahedra form 1D ribbons two octahedra wide (Fig. 1). This two octahedra subunit is bridged by both μ_2 and μ_3 thiocyanate ligands to the next double octahedron subunit. This configuration produces

Table 1 Lattice parameters for compounds **1–4** from single crystal X-ray diffraction

	CPACd $(SCN)_2Cl$ (**1**)	CPACd $(SCN)_2Br$ (**2**)	IBACd $(SCN)_2Cl$ (**3**)	IPACd $(SCN)_2Cl$ (**4**)
T (K)	298	298	100	100
Space group	$P\bar{1}$	$P\bar{1}$	$P\bar{1}$	$P\bar{1}$
a (Å)	5.9082(4)	5.9164(6)	5.9664(3)	5.8644(2)
b (Å)	10.2084(8)	9.822(1)	9.2609(4)	9.7409(4)
c (Å)	11.4671(8)	11.875(2)	11.1509(5)	12.1164(5)
α (°)	113.822(2)	99.211(4)	87.173(2)	79.447(1)
β (°)	99.670(2)	103.298(4)	83.075(2)	78.168(1)
γ (°)	90.293(2)	98.195(4)	79.658(1)	79.137(1)
V (Å^3)	621.66(8)	651.2(1)	601.46(5)	657.74(4)

Table 2 Selected bond lengths and angles of compounds **1–4**. The labels μ_2-S and μ_3-S refer to sulfur on the μ_2-SCN^- and the μ_3-SCN^-, respectively, and X refers to the halide ion (Cl or Br)

	$CPACd(SCN)_2Cl$ (**1**)	$CPACd(SCN)_2Br$ (**2**)
Cd–X (Å)	2.580(2)	2.683(1)
Cd–μ_2-S (Å)	2.669(1)	2.633(2)
Cd–μ_3-S (Å)	2.8066(9), 2.826(1)	2.808(2), 2.924(1)
Cd–N (Å)	2.265(4), 2.298(4)	2.254(5), 2.318(5)
Cd–N–C (°)	159.5(4), 167.2(4)	153.7(5), 165.8(6)
Cd–μ_2-S–C (°)	98.8(1)	98.9(2)
Cd–μ_3-S–C (°)	99.2(1), 100.6(1)	101.7(2), 102.1(1)
Cd–S–Cd (°)	96.19(4)	100.63(5)
X–H_A (Å), N–H–X (°)	2.389(1), 150.7(4)	2.4581(7), 170.9(4)
	2.397(1), 153.8(3)	2.5274(8), 151.8(4)
	2.416(1), 155.3(4)	2.9968(8), 117.7(4)
	$IBACd(SCN)_2Cl$ (**3**)	$IPACd(SCN)_2Cl$ (**4**)
Cd–X (Å)	2.5399(7)	2.5615(6)
Cd–μ_2-S (Å)	2.6371(8)	2.6385(7)
Cd–μ_3-S (Å)	2.7144(7), 2.9786(7)	2.7756(6), 2.9303(6)
Cd–N (Å)	2.272(3), 2.332(3)	2.260(2), 2.314(2)
∠Cd–N–C (°)	153.1(1), 160.8(3)	154.0(2)
∠Cd–μ_2-S–C (°)	99.58(9)	98.23(8)
∠Cd–μ_3-S–C (°)	101.66(8), 103.13(7)	104.16(7)
∠Cd–S–Cd (°)	99.48(3)	97.38(2)
X–H_A (Å), N–H–X (°)	2.3427(7), 165.8(1)	2.3253(5), 171.7(1)
	2.4703(8), 141.7(2)	2.3507(5), 155.0(1)
	2.8341(8), 116.8(1)	2.7940(5), 110.7(1)

slightly distorted octahedra with the Cd shifted away from the shared edge, resulting in three unique Cd–S and two unique Cd–N bond lengths.

Although the packing of the organic amines slightly changes depending on the length and connectivity of the hydrocarbon tails, nearly the same hydrogen bonding pattern is observed in compounds **1–4**. The amines occupy the space between the chains, with the amine heads oriented to form three interactions that hold the inorganic and organic components together. In compound **1**, $CPACd(SCN)_2Cl$, there are three hydrogen bonds to the chloride ligands; two nearly equivalent shorter hydrogen bonds to chlorides within the same chain and one slightly longer hydrogen bond to a chloride in the neighboring chain (Fig. 2). In compounds **2–4** this pattern changes slightly as the relative positions of the inorganic chains shift. This causes the hydrogen bonds to the halide ions within the same chain to become inequivalent. More importantly it changes the interaction to the neighboring chain from a discrete hydrogen bond to a diffuse attraction to the three anions (X^-, SCN^-, and NCS^-) on one face of the octahedron.

Disorder of the hydrocarbon tails of the isobutylammonium and isopentylammonium ions prevented full structure solution at room temperature, necessitating scans at 100 K. For compound **4** containing isopentylammonium the structure still showed rotational disorder at the α-CH_2 position at 100 K, with the final structure being a superposition of two rotational confomers. This type of disorder has previously been observed in the compositionally similar compounds IBA_2CdBr_4 and IPA_2CdCl_4.[33,34] In all cases the tail of the amine points towards the thiocyanate linkers on the inorganic chains.

SCXRD of the irregular clear crystals of compound **5** shows that the inclusion of the larger benzylammonium cation increases the size of the inorganic ribbons. Although bridging still occurs through thiocyanate ions, the ribbons are now three octahedra wide with two chemically inequivalent Cd ions (Fig. 3). Within this three octahedra assembly the central octahedron is made up of a Cd ion coordinated by two *trans*-oriented NCS^- ligands and four SCN^- ligands where the sulfur atom is shared with the one of the outer Cd octahedra. The outer Cd-centered octahedra contain both SCN^- and Cl^- ligands with three SCN^- ligands in the *mer* orientation, two *trans* NCS^- ligands, and a single terminal Cl^- ion. Similar to compounds **1–4** the outer

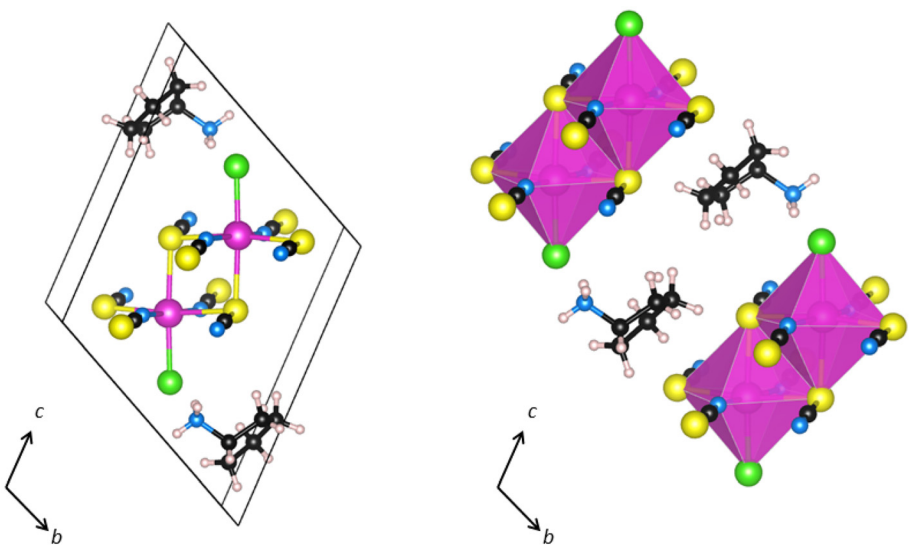

Fig. 1 Two views of the structure of $CPACd(SCN)_2Cl$, representative of compounds **1–4**, viewed looking down the thiocyanate ribbons. The atoms shown are represented by the colors Cd-magenta, Cl-green, S-yellow, C-black, N-blue, and H-white.

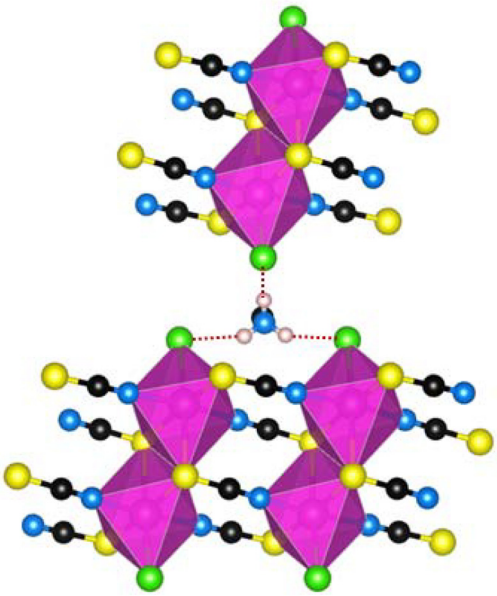

Fig. 2 Hydrogen bonding environment of cyclopentylammonium in compound **1**. Only the NH_3 head group of the cyclopentylammonium cation is shown for clarity. Hydrogen bonds are shown as red dotted lines. The atoms shown are represented by the colors Cd-magenta, Cl-green, S-yellow, C-black, N-blue, and H-white.

Cd ions are displaced away from the shared edge. The expansion of the inorganic moiety also expands the unit cell and introduces new symmetry elements changing the space group symmetry to $P2_1/n$. Compound **6**, which also contains benzylammonium, returns to the inorganic structure of compounds **1–4** with ribbons two octahedra wide, presumably due to incorporation of the larger bromide ion. Structural details for compounds **5–7** are given in Tables 3 and 4 with further information given in the SI (Table S2).

Table 3 Lattice parameters of compounds **5–7** from single crystal X-ray diffraction

	$BzA_2Cd_3(SCN)_6Cl_2$ (**5**)	$BzACd(SCN)_2Br$ (**6**)	$Ani_2Cd(SCN)_2Br_2$ (**7**)
T (K)	298	298	298
Space group	$P2_1/n$	$P\bar{1}$	$C2/c$
a (Å)	12.792(2)	5.8458(3)	22.100(2)
b (Å)	5.8894(7)	10.1305(6)	7.8037(7)
c (Å)	21.896(3)	12.1382(6)	11.0731(8)
α (°)	90	79.520(2)	90
β (°)	101.592(4)	80.742(2)	94.037(5)
γ (°)	90	76.902(2)	90
V (Å^3)	1615.9(4)	683.06(6)	1905.0(3)

Single crystal X-ray diffraction of the rhombohedral, bladed crystals of $Ani_2Cd(SCN)_2Br_2$ reveals yet another structural modification, one made up of one-dimensional chains of octahedra, with each octahedron bridged by thiocyanate ligands to another octahedron along the chain. Within the octahedron the two Br^- ligands and the two N-bonded NCS^- ligands are *cis* oriented, while the S-bonded SCN^- ligands are *trans* coordinated. An inversion center lies along the inorganic chain midway between two octahedra. Consequently, the two *cis*-coordinated ligands alternate upon translating along the *b* axis (Fig. 4). Bond lengths and angles within the octahedron are shown in Table 4. The protonated anilinium cations are situated in the space above and below each inorganic chain with the ammonium head group being slightly offset above or below the plane of the bromide ligands. The centroids of the aromatic rings form a parallelogram with parallel rings slip stacked and the adjacent rings that are oriented edge-to-edge in a T-shape. The anilinium cation is oriented so that it forms two hydrogen bonds to bromide ligands on octahedra in neighboring chains with nearly identical lengths. The third hydrogen of the amine forms a weaker electrostatic interaction with the nitrogen end of the bridging NCS^- ligand.

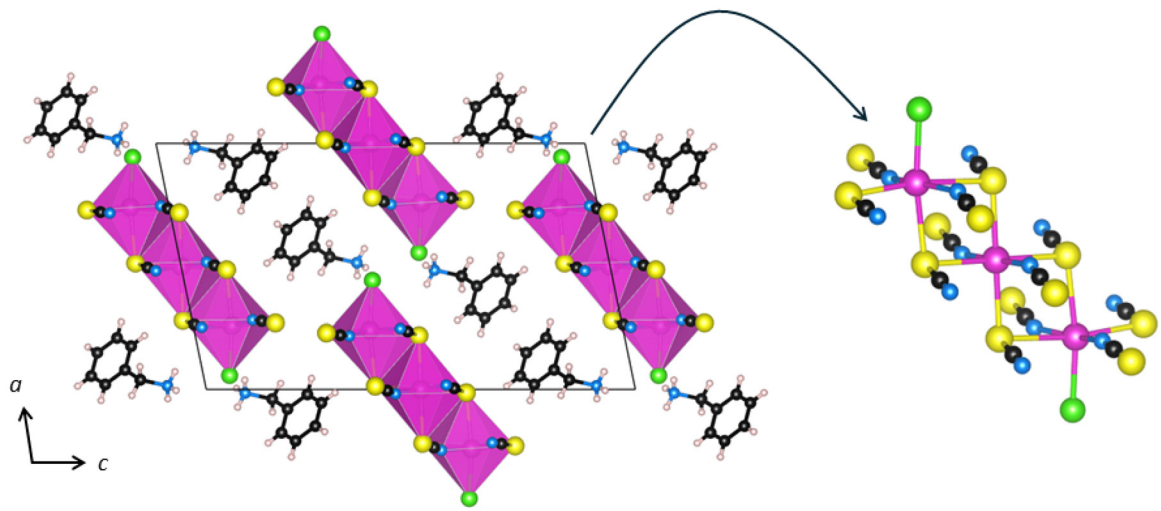

Fig. 3 Two views of the structure of $BzA_2Cd_3(SCN)_6Cl_2$ showing the three octahedra subunit, viewed down the axis of the bridging thiocyanates. The atoms shown are represented by the colors Cd-magenta, Cl-green, S-yellow, C-black, N-blue, and H-white.

Table 4 Selected bond lengths and angles of compounds **5–7**

	$BzA_2Cd_3(SCN)_6Cl_2$ (**5**)	$BzACd(SCN)_2Br$ (**6**)	$Ani_2Cd(SCN)_2Br_2$ (**7**)
Cd–X (Å)	2.539(1)	2.6763(7)	2 × 2.6902(4)
Cd–μ_2-S (Å)	2.640(1)	2.638(1)	2 × 2.7214(6)
Cd–μ_3-S (Å)	2.744(1), 2.761(1), 2.863(1), 2.958(1)	2.792(1), 2.919(1)	—
Cd–N (Å)	2.238(4), 2.257(4), 2.305(4)	2.266(4), 2.307(3)	2 × 2.406(3)
∠Cd–N–C (°)	155.9(3), 160.4(3), 169.0(4)	147.4(4), 152.6(4)	132.9(2)
∠Cd–μ_2-S–C (°)	97.3(1)	99.4(1)	102.11(8)
∠Cd–μ_3-S–C (°)	99.5(2), 99.6(1), 100.6(1)	100.1(1), 106.2(1)	
∠Cd–S–Cd (°)	96.21(3), 98.05(3)	96.78(4)	
X–H_A (Å), ∠N–H–X (°)	2.305(1), 159.2(3) 2.516(1), 134.9(3) 2.858(1), 106.5(4)	2.4254(5), 167.7(3) 2.4803(6), 156.8(3) 3.1272(5), 100.2(3)	2.4135(3), 169.4(1) 2.4137(3), 160.5(1)

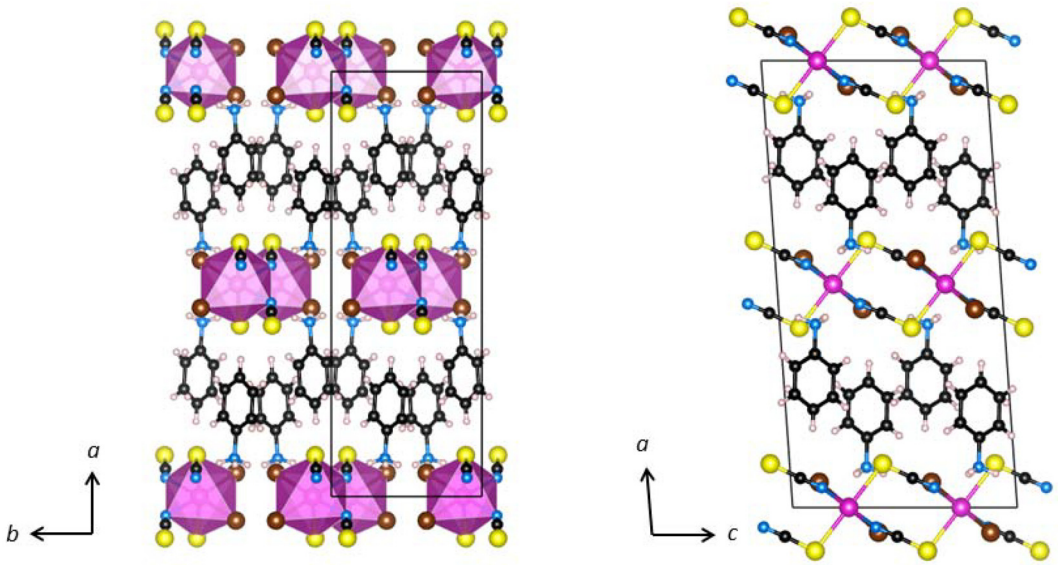

Fig. 4 Crystal structure of $Ani_2Cd(SCN)_2Br_2$ viewed down the *c*-axis (left) and *b*-axis (right). The atoms shown are represented by the colors Cd-magenta, Br-maroon, S-yellow, C-black, N-blue, and H-white.

Electronic structure

Band structure diagrams and partial density of states were calculated for representative compounds **1** and **2** using density functional theory and are shown in Fig. 5 and 6. The indirect bandgaps for these compounds were calculated to be 3.74 and 3.53 eV respectively, however, the direct bandgaps were only slightly larger at 3.79 and 3.63 eV. The partial density of states shows that in all cases the conduction band minimum (CBM) is made up of Cd 5s-orbitals while the valence band maximum (VBM) is made up of largely of sulfur 3p-orbitals with some nitrogen 2p contribution, while the halide p-orbitals lie directly below the VBM. The Br orbitals are slightly higher in energy than the Cl orbitals, overlapping to a greater extent with the S orbitals making up the VBM. While the bands are largely flat there is some dispersion in the lowest energy conduction bands that are derived from cadmium 5s orbitals. The band widths range from 0.53 to 0.80 eV from the Γ to V points for compounds **1** and **2** respectively.

Diffuse reflectance UV-vis data were also collected for all compounds (Fig. 7 and S2). The optical bandgaps were estimated using the Tauc method and found to vary from 4.33 eV to 4.57 eV (Table S3). Given that the DFT calculations show ≤0.1 eV difference in indirect and direct bandgap energies, a direct transition was assumed to be the major contributor to the bandgap for the Tauc method. Bandgaps for the bromide compounds were consistently a few tenths of an eV smaller than their chloride counterparts, for example 4.54 eV and 4.33 eV for compounds **1** and **2**, respectively. Optical transitions for the benzylammonium and anilinium compounds are equivalent to the transitions measured for the amine salts. Tauc plots and DRS data can be found in the SI.

Discussion

The synthesis approach employed in this study consistently resulted in a specific stoichiometry independent of whether a

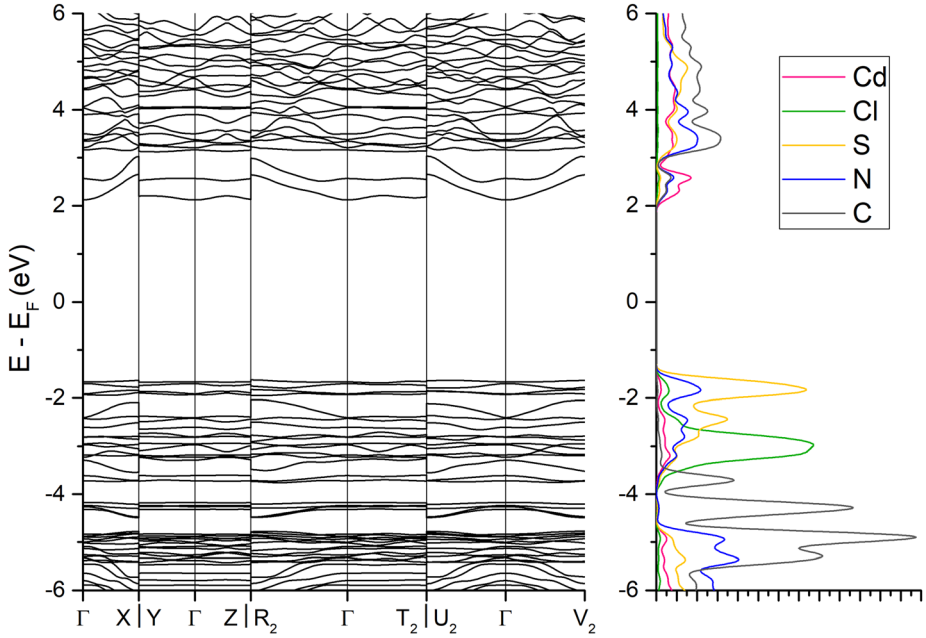

Fig. 5 Band structure and partial density of states for compound **1** showing an indirect band gap of 3.74 eV between Z and Γ and a direct band gap of 3.79 eV at Γ.

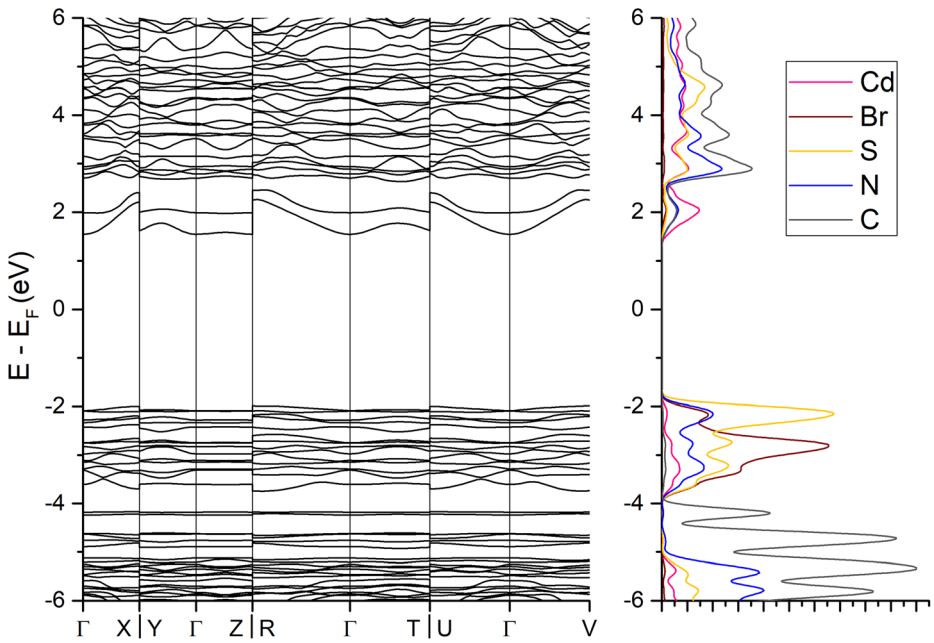

Fig. 6 Band structure and partial density of states for compound **2** showing an indirect band gap of 3.53 eV between V and Γ and a direct band gap of 3.63 eV at Γ.

1 : 1, 2 : 1, or 2 : 3 ratio of the starting materials was used. Under these synthetic conditions only reactions utilizing Cd^{2+} produced compounds of the structure type reported herein. Identical reactions involving other divalent metals (Ni^{2+}, Co^{2+}, Fe^{2+}, Mn^{2+}, and Zn^{2+}) with the amine salts that were a part of this study did not produce similar compositions, indicating that Cd^{2+} is uniquely able to form these types of thiocyanate-bridged structures. The differing halide-to-thiocyanate ratios, driven by the choice of amine salt, determine the connectivity and dimensionality of the inorganic fragment of each compound. The change from chains that are one octahedron wide for anilinium to ribbons that are two or three octahedra wide for the other organic cations is presumably driven by the need to optimize the noncovalent interactions between organic

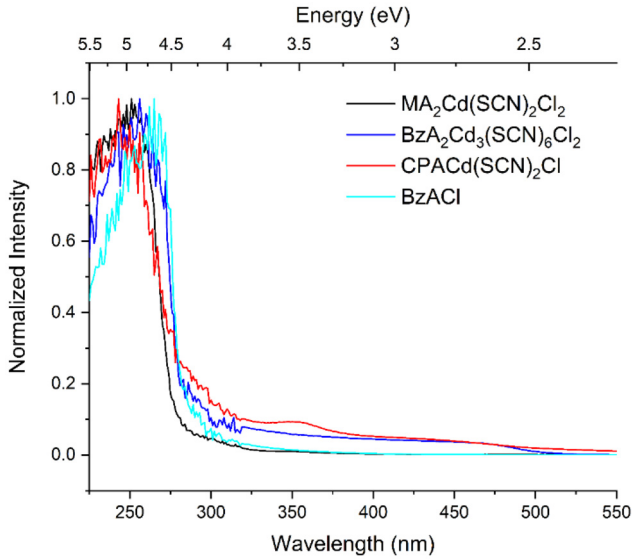

Fig. 7 Comparison of DRS data for thiocyanate halides with 1D chains that are one ($MA_2Cd(SCN)_2Cl_2$), two ($CPACd(SCN)_2Cl$), and three ($BzA_2Cd_3(SCN)_6Cl_2$) octahedral subunits wide, as well as for benzylammonium chloride. Data has been transformed to pseudoabsorbance using the Kubelka–Munk method and normalized by maximum absorbance.

cations. Thus, understanding the interplay between the structural influences of the halide ion and the organic cation, including potential π–π interactions between aromatic rings, allows for tunable and directed synthesis of these hybrid thiocyanate-halide materials with different structure types.

Compounds **1–6** can be understood structurally as being on a spectrum that ranges from 1D chains that are a single octahedron wide, as seen for $A_2Cd(SCN)_2Cl_2$ ($A = CH_3(CH_2)_nNH_3^+$ with n = 0–3), to the three-dimensional binary material $Cd(SCN)_2$ from which these compounds are made (Fig. 8).[23,35] The protonated amine halide salt acts as a scissor, cleaving the 3D cadmium thiocyanate framework into smaller units. These units are terminated by halide ions that form strong hydrogen bonds with the organic cation. As the size of the organic cation increases, the Cd-centered octahedra form edge-sharing clusters through bridging μ_3-sulfur atoms of the thiocyanate group. This increases the width of the 1D chain, presumably to better match with the increasing size of the organic cation (Table 5).

With smaller organic cations, such as the previously reported series of linear primary ammonium type cations ($CH_3(CH_2)_nNH_3^+$ n = 0–3) and $Ani_2Cd(SCN)_2Br_2$, the observed ratio of $Cd(SCN)_2$ to amine halide salt (AX) to is 1 : 2. This stoichiometry gives rise to 1D chains built up from a Cd-centered octahedron bridged by both the sulfur and nitrogen ends of the thiocyanate anion forming μ_2 linkers. The bulkier IBA, IPA, and CPA protonated amines (as measured by van der Waals volume) stabilize a $Cd(SCN)_2$ to AX ratio of 1 : 1 forming one-dimensional inorganic frameworks made up of two edge-sharing Cd^{2+} octahedra that are bridged by SCN^- ions to form ribbons. The structural building unit is now two Cd-centered

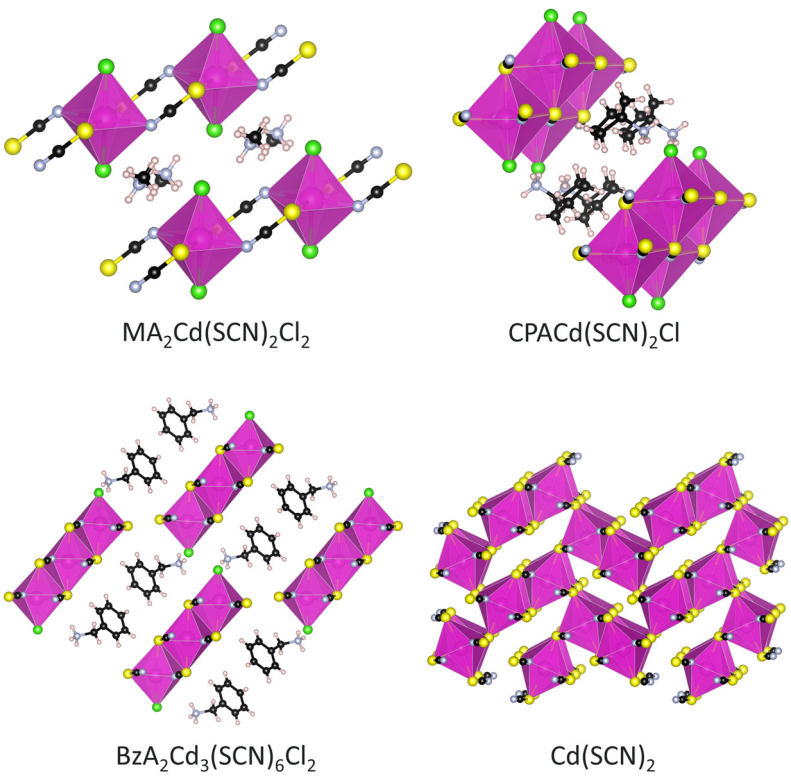

Fig. 8 Structural evolution of hybrid thiocyanate-halides to $Cd(SCN)_2$.

Table 5 Comparison of amine sizes from this and previous reports with the number of cations incorporated and the resulting number of octahedral subunits

Unprotonated amine	van der Waals volume (Å^3)	Octahedra in building unit	$Cd(SCN)_2$/ACl ratio
Methylamine–butylamine[23]	40.16–91.05	1	1 : 2
Aniline[36]	93.01	1	1 : 2
Isobutylamine	91.21	2	1 : 1
Cyclopentylamine	96.49	2	1 : 1
Isopentylamine	108.22	2	1 : 1
Benzylamine	110.79	3	3 : 2

octahedra that share a common edge. In one edge-sharing cluster six of the SCN^- ions are μ_2 linkers that only bridge one cluster to the next, while the other two are μ_3 linkers where the sulfur end forms the shared edge and the nitrogen end bridges to the next cluster. The Cd–μ_3-S bonds are consistently longer than Cd–μ_2-S bonds in all of these compounds, as would be expected.

When the larger benzylammonium cation is incorporated, the ratio again increases to 3 : 2 and as a result the inorganic ribbons are now built up from a cluster of three Cd-centered octahedra sharing common edges. The central octahedron is coordinated exclusively by μ_3 thiocyanate linkers, four *via* the sulfur end making up both the shared edges and two *via* the nitrogen end forming bridges to the next cluster. The outer octahedra are made up of three μ_3-SCN^- linkers and two μ_2-SCN^- linkers with the shared edges always being made up of sulfur atoms.

The structures that contain ribbons resemble $Cd(SCN)_2$, a 3D structure built from a pair of Cd-centered octahedra that share a common edge. The octahedra are formed by four sulfur bonded μ_3-SCN^- linkers and two nitrogen bonded μ_2-SCN^- linkers. The similarity in connectivity is supported by similar bond angles as well. The Cd–μ_2-S–C and Cd–μ_3-S–C bond angles in the hybrid compounds range from 97.48–99.52° and 98.23–106.34° respectively, and Cd–N–C angles range from 147.6–168.6°. These values are similar to those seen in $Cd(SCN)_2$ where the Cd–S–C angles range from 98.2–99.1° and the Cd–N–C angles from 163.6–166.0°. These similarities arise from the local bonding of the thiocyanate to Cd^{2+}, where the Cd–N–C bond angles are close to linear to optimize the bonding interaction between the nitrogen lone pair and cadmium. The Cd–S–C bond angles fall within a narrow range between 90–110°. A structural feature that is consistent across a wide range of cadmium thiocyanates.[13,37,38]

What sets these materials apart from the binary $Cd(SCN)_2$ is the introduction of halide ions which exclusively adopt a terminal configuration in the cadmium octahedron, breaking apart the 3D structure of $Cd(SCN)_2$ and reducing the dimensionality. The terminal halide configuration facilitates the formation of strong hydrogen bonds between the halide anion and ammonium head group of the organic cation. This pattern of hydrogen bonding binds the amine group to the inorganic framework and is maintained in all structures reported here. It also imposes constraints on the manner in which the organic cations can be packed around the inorganic chains. As the size of the organic cation increases the width of the inorganic 1D chains must also increase, resulting in an increase in the $Cd(SCN)_2$ to AX ratio.

The packing of the organic cations is affected not only by steric considerations but also by other non-covalent interactions, particularly for the aromatic cations benzylammonium and anilinium. Even though the benzylammonium cations are only slightly larger than the isopentylammonium cations, the addition of benzylic π interactions drives the expansion of the inorganic ribbons to three octahedra wide in compound **5**. In this composition the BzA cations are oriented such that they have slip stacking, characterized by a centroid-to-centroid distance of 5.889 Å, and T-shaped edge to face interactions, with a centroid to centroid distance of 5.145 Å, (Fig. 9) both of which are energetically favorable benzylic π interactions as explored by Oberle *et al.*[39] The rigidity of the BzA cations leads to an expansion in the width of the inorganic ribbons, all while maintaining the two hydrogen bonds and one diffuse interaction, as also seen in compounds **2–4**.

In compound **6**, where the BzACl is replaced by BzABr, the competing effects of hydrogen bonding to the now larger halide and the π interactions complicate the picture. In this compound the benzylammonium cations adopt the combination of slip-stacking, with a 5.846 Å centroid-to-centroid distance, and less favorable edge-to-edge interactions (Fig. 9), resulting in a 1 : 1 AX : $Cd(SCN)_2$ ratio and ribbons two octahedra wide. The slip stacking arrangement is nearly identical in both benzylammonium compounds, with very similar centroid-to-centroid distances of 5.889 and 5.846 Å, maintaining the strongest set of favorable interactions observed in similar organic compounds containing benzylammonium.[39]

The combined effects of hydrogen bonding, steric repulsion, and π-interactions come to a head in compound **7**, $Ani_2Cd(SCN)_2Br_2$, which sees a 1 : 2 ratio of $Cd(SCN)_2$ to AX despite an organic volume (93.01 Å^3) akin to cyclopentylammonium (96.49 Å^3). This compound is also isostructural to $Ani_2Cd(SCN)_2Cl_2$ reported by Jabbar *et al.*,[36] showing that in this case the relative size or strength of the hydrogen bond to the halide is not the only reason for the structural change. The anilinium cations form an offset bilayer resulting from a combination of energetically favorable slip-stacking and T-shaped edge-to-face interactions, similar to the arrangement of amines in the one-dimensional compound $Ani_4Cd_3Br_{10}$.[40] The conformational rigidity of anilinium leads to a structure where the inorganic framework is built up from a single Cd-centered octahedron, similar to $A_2Cd(SCN)_2Cl_2$ (A = $CH_3(CH_2)_nNH_3^+$, n = 0–3) except that the halide ions are *cis* coordinated instead of *trans* coordinated within each octahedron. This change allows for the anilinium cation to form two hydrogen bonds to the halide ions in neighboring inorganic chains, while also maximizing the π-interactions. This *cis* coordination of the halide ions within 1D cadmium thiocyanate-halide chains is unusual, but has previously been observed in $(C_2H_{10}N_2)Cd(SCN)_2Cl_2$.[41] The structure of the anilinium bilayer is such that ammonium

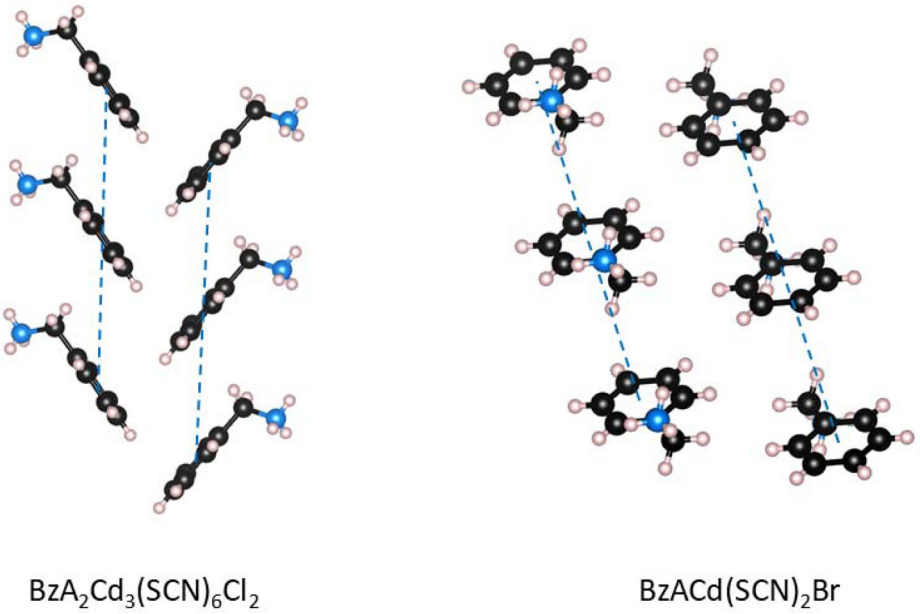

Fig. 9 Packing of benzylammonium cations in compound **5** showing slip stacking in the vertical direction and edge-to-face in the horizontal direction (left). The packing in compound **6** also exhibits slip stacking in the vertical direction but differs in the horizontal direction where edge-to-edge packing is observed (right). In both images the centroid-to-centroid distance along the slip stacking directions are marked with blue dotted lines. Inorganic chains omitted for clarity.

head group on neighboring cations point in opposite directions, similar to the diamine in $(C_2H_{10}N_2)Cd(SCN)_2Cl_2$. The *cis* configuration in both of these compounds brings the hydrogen bond acceptors closer together, allowing each set of two donor groups to form a hydrogen bond with the halides on two separate chains (Fig. 10).

The changes in the inorganic fragments seen across these compounds seem to have a minimal impact on the electronic structures of these materials. Although the VBM and CBM in these compounds are made up of sulfur and cadmium orbitals respectively, altering the width of the cadmium thiocyanate 1D fragment has minimal impact on the band gap or band curvature, which leads to the conclusion that these materials have electronic structures that are nearly zero-dimensional in character. The greatest curvature in this family occurs in the conduction band between the Γ and V points with a magnitude of 0.5–0.8 eV, which is considerably less than that observed in the two-dimensional, halide-bridged $MA_2Pb(SCN)_2I_2$ and $MA_2Sn(SCN)_2Cl_2$.[22,42] The small increase in the band gap of 0.3 eV in the comparable chloride and bromide compositions, **1** and **2**, likely arises due greater hybridization of the Cd 5s orbitals with the Br 4p orbitals compared to the Cl 3p orbitals.

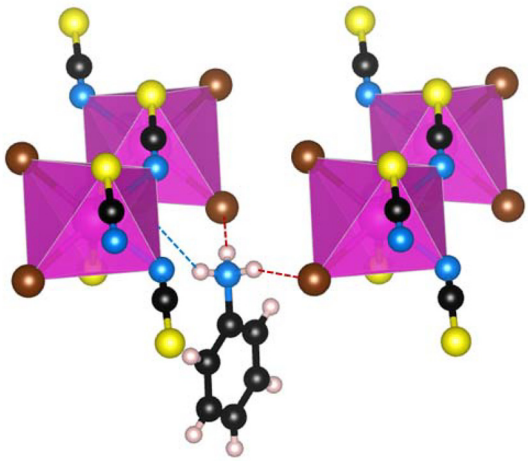

Fig. 10 Hydrogen bonding environment of anilinium in compound **7**. Hydrogen bonds are shown as red dotted lines, and the diffuse interaction is shown as a blue dashed line.

Despite the isolated electronic nature of the inorganic octahedra, the flexibility of the cadmium thiocyanate inorganic framework offers the opportunity to incorporate optically interesting organic cations. The absorption onsets of compounds **1–4** arise from the transitions between the sulfur 3p-orbitals and cadmium 5s-orbitals, a feature common to all seven compounds. The magnitude of the resulting band gap (E_g > 4.3 eV) is large enough to accommodate optically active organic cations without interference. Further the absorption can be tuned by changing the halide ion as the observed band gap is consistently smaller for the bromide-containing compounds than it is for the chloride-containing compounds.

Conclusion

Seven hybrid halide-thiocyanate compounds are reported herein utilizing bulky cyclic, aromatic, or branched chain

amines as organic cations. The ability of cadmium to bond to either end of the thiocyanate ion favors structures that feature bridging thiocyanate ligands and terminal halide ions. This leads to inorganic substructures that contain 1D chains or ribbons. As the size and bulkiness of the organic cation increases, the width of the inorganic chain/ribbon increases and the AX to $Cd(SCN)_2$ ratio decreases. In this way the inorganic fragment accommodates larger organic cations while maintaining strong hydrogen bonding interactions with the terminal halide groups. In all cases the halide ions adopt terminal positions within the inorganic fragments thereby acting as scissors to break up the 3D connectivity seen in $Cd(SCN)_2$.

When the organic cation is anilinium the SCN^- coordinates one Cd^{2+} ion at the nitrogen end and another Cd^{2+} ion at the sulfur end (μ_2 coordination). This results in an inorganic fragment featuring 1D chains a single octahedron wide, with the halide ions in a *cis* coordination. The other six compounds contain ribbons built up from octahedra that share edges through the sulfur end of the SCN^- ligand (μ_3 coordination). In $BzA_2Cd_3(SCN)_6Cl_2$ the ribbons are built from clusters of three octahedra sharing common edges, while in the other compositions the ribbons are built from two octahedra that share a common edge. This study shows how the malleability of Cd^{2+} thiocyanates allows for the formation of hybrid compounds that incorporate a wide range of organic cations.

Author contributions

A. M. carried out experimental and computational work. Both authors contributed to the conception of the research and writing the manuscript.

Conflicts of interest

The authors declare no conflicts of interest.

Data availability

Details are available as supporting data in the supplementary information (SI). Supplementary information: details of amines used (S1), DRS data (S2), Tauc plots (S3–S9), PXRD data (S10–16), and further SCXRD refinement information. See DOI: https://doi.org/10.1039/d6dt00207b.

CCDC 2454582–2454588 contain the supplementary crystallographic data for this paper.[43a–g]

Acknowledgements

The authors jointly acknowledge the National Science Foundation for funding this work under grant DMR-2003793 and thank the X-ray Crystallography Facility at The Ohio State University for the use of single crystal X-ray diffractometers.

References

1 J. D. Sosa, T. F. Bennett, K. J. Nelms, B. M. Liu, R. C. Tovar and Y. Liu, Metal–Organic Framework Hybrid Materials and Their Applications, *Crystals*, 2018, **8**, 1–23, DOI: 10.3390/cryst8080325.

2 A. K. Cheetham and C. N. R. Rao, There's Room in the Middle, *Science*, 2007, **318**, 58–59, DOI: 10.1126/science.1147231.

3 A. E. Maughan, A. M. Ganose, A. M. Candia, J. T. Granger, D. O. Scanlon and J. R. Neilson, Anharmonicity and Octahedral Tilting in Hybrid Vacancy-Ordered Double Perovskites, *Chem. Mater.*, 2018, **30**, 472–483, DOI: 10.1021/acs.chemmater.7b04516.

4 W. Li, Z. Wang, F. Deschler, S. Gao, R. H. Friend and A. K. Cheetham, Hybrid Perovskites; New Opportunities beyond Oxides Wei, *Nat. Rev. Mater.*, 2017, **2**, 16099.

5 G. Kieslich, S. Sun and A. K. Cheetham, An Extended Tolerance Factor Approach for Organic-Inorganic Perovskites, *Chem. Sci.*, 2015, **6**, 3430–3433, DOI: 10.1039/c5sc00961h.

6 H. L. B. Boström, M. S. Senn and A. L. Goodwin, Recipes for Improper Ferroelectricity in Molecular Perovskites, *Nat. Commun.*, 2018, **9**, 1–7, DOI: 10.1038/s41467-018-04764-x.

7 M. J. Cliffe, E. N. Keyzer, A. D. Bond, M. A. Astle and C. P. Grey, The Structures of Ordered Defects in Thiocyanate Analogues of Prussian Blue, *Chem. Sci.*, 2020, **11**, 4430–4438, DOI: 10.1039/d0sc01246g.

8 S. Kronawitter and G. Kieslich, The Wondrous World of ABX_3 Molecular Perovskites, *Chem. Commun.*, 2024, 11673–11684, DOI: 10.1039/d4cc03833a.

9 A. Abuduheni, N. Yisimayili, H. Hu, Y. Yan, Y. Liu and Z. Liu, Isostructural Phase Transition and Dielectric Reversibility in a Cobalt Thiocyanate Complex Incorporating an Organic-Inorganic Hybrid Compound: $(C_5H_7N_2)_2[Co(NCS)]_4$, *J. Mol. Struct.*, 2024, **1318**, 139267, DOI: 10.1016/j.molstruc.2024.139267.

10 M. J. Cliffe, Inorganic Metal Thiocyanates, *Inorg. Chem.*, 2024, **63**, 13137–13156, DOI: 10.1021/acs.inorgchem.4c00920.

11 G. Thiele and D. Messer, S–Thiocyanato– Und N–Isothiocyanato–Bindungsisomerie in Den Kristallstrukturen von $RbCd(SCN)_3$ Und $CsCd(SCN)_3$, *Z. Anorg. Allg. Chem.*, 1980, **464**, 255–267, DOI: 10.1002/zaac.19804640124.

12 C. Wechwithayakhlung, D. M. Packwood, D. J. Harding and P. Pattanasattayavong, Structures, Bonding, and Electronic Properties of Metal Thiocyanates, *J. Phys. Chem. Solids*, 2021, **154**, 110085, DOI: 10.1016/j.jpcs.2021.110085.

13 J. Y. Lee, S. Ling, S. P. Argent, M. S. Senn, L. Cañadillas-Delgado and M. J. Cliffe, Controlling Multiple Orderings in Metal Thiocyanate Molecular Perovskites $A_x\{Ni[Bi(SCN)_6]\}$, *Chem. Sci.*, 2021, **12**, 3516–3525, DOI: 10.1039/d0sc06619b.

14 B. Guo, X. Zhang, Y. N. Wang, J. J. Huang, J. H. Yu and J. Q. Xu, New 1-D and 3-D Thiocyanatocadmates Modified by Various Amine Molecules and Cl^-/CH_3COO^- Ions: Synthesis, Structural Characterization, Thermal Behavior

and Photoluminescence Properties, *Dalton Trans.*, 2015, **44**, 5095–5105, DOI: 10.1039/c4dt03799e.

15 L. He, L. Zhou, P. P. Shi, Q. Ye and D. W. Fu, One-Dimensional Cadmium Thiocyanate Perovskite Ferroelastics Tuned by Halogen Substitution, *Chem. Mater.*, 2019, **31**, 10236–10242, DOI: 10.1021/acs.chemmater.9b04232.

16 W. X. Zhang, S. L. Chen, Y. Shang, Z. H. Yu and X. M. Chen, Molecular Perovskites as a New Platform for Designing Advanced Multi-Component Energetic Crystals, *Energ. Mater. Front.*, 2020, **1**, 123–135, DOI: 10.1016/j.enmf.2020.12.003.

17 K. P. Xie, W. J. Xu, C. T. He, B. Huang, Z. Y. Du, Y. J. Su, W. X. Zhang and X. M. Chen, Order-Disorder Phase Transition in the First Thiocyanate-Bridged Double Perovskite-Type Coordination Polymer: $[NH_4]_2[NiCd(SCN)_6]$, *CrystEngComm*, 2016, **18**, 4495–4498, DOI: 10.1039/c6ce00898d.

18 S. Ramkumar and P. Malliga, Centrosymmetric Crystal Structure and Third Order Nonlinear Optical Properties of $[2(C_{10}H_{20}O_5)NH_4][Cd(SCN)_3]$: CCTC Single Crystal for Optical Application, *Opt. Quantum Electron.*, 2023, **55**, 1–20, DOI: 10.1007/s11082-023-05432-1.

19 Y. Dang, G. Liu, J. Song, L. Meng, Y. Sun, W. Hu and X. Tao, Layered Perovskite $(CH_3NH_3)_2Pb(SCN)_2I_2$ Single Crystals: Phase Transition and Moisture Stability, *ACS Appl. Mater. Interfaces*, 2020, **12**, 37713–37721, DOI: 10.1021/acsami.0c09251.

20 Q. Jiang, D. Rebollar, J. Gong, E. L. Piacentino, C. Zheng and T. Xu, Pseudohalide-Induced Moisture Tolerance in Perovskite $CH_3NH_3Pb(SCN)_2I$ Thin Films, *Angew. Chem., Int. Ed.*, 2015, **54**, 7617–7620, DOI: 10.1002/anie.201503038.

21 Y. Numata, Y. Sanehira, R. Ishikawa, H. Shirai and T. Miyasaka, Thiocyanate Containing Two-Dimensional Cesium Lead Iodide Perovskite, $Cs_2PbI_2(SCN)_2$: Characterization, Photovoltaic Application, and Degradation Mechanism, *ACS Appl. Mater. Interfaces*, 2018, **10**, 42363–42371, DOI: 10.1021/acsami.8b15578.

22 S. Karoui, H. Chouaib and S. Kamoun, Synthesis, Crystal Structure and Phase Transition in a Perovskite Type $(CH_3NH_3)_2M(X)_2(Y)_2$(M=Sn; X=SCN; Y=Cl), *J. Mol. Struct.*, 2022, **1253**, 132206, DOI: 10.1016/j.molstruc.2021.132206.

23 A. Milder, T. Liu and P. M. Woodward, Structure Directing Influences in a Family of One-Dimensional Hybrid Cadmium Thiocyanate Halides, *Inorg. Chem.*, 2025, **64**, 18135–18143, DOI: 10.1021/acs.inorgchem.5c01639.

24 B. Guo, X. Zhang, J. H. Yu and J. Q. Xu, New Organically Templated Thiocyanatocadmates and Chlorocuprate(II): Synthesis and Structural Characterization, *Dalton Trans.*, 2015, **44**, 11470–11481, DOI: 10.1039/c5dt01355k.

25 C. H. Wang, L. Li, H. J. Du, W. L. Zhang, Y. Li, Y. Y. Niu and Y. Fu, Five Hybrid Thiocyanate Networks Oriented by Polyvalent Cationic Templates: Synthesis, Structure and Properties, *Inorg. Chim. Acta*, 2015, **437**, 1–10, DOI: 10.1016/j.ica.2015.07.046.

26 H. L. Jia, M. J. Jia, H. Ding, J. H. Yu, J. Jin, J. J. Zhao and J. Q. Xu, New Thiocyanatocadmates with Bidentate N-Heterocyclic Molecules as the Templating Agents: Synthesis and Structural Characterization, *CrystEngComm*, 2012, **14**, 8000–8009, DOI: 10.1039/c2ce26164b.

27 Bruker, *SAINT*, Bruker AXS Inc., Madison, Wisconsin, USA, 2012.

28 G. M. Sheldrick, *SADABS*, University of Göttingen, Germany, 1996.

29 G. M. Sheldrick, SHELXT - Integrated Space-Group and Crystal-Structure Determination, *Acta Crystallogr., Sect. A: Found. Adv.*, 2015, **71**, 3–8, DOI: 10.1107/S2053273314026370.

30 O. V. Dolomanov, L. J. Bourhis, R. J. Gildea, J. A. K. Howard and H. Puschmann, OLEX2: A Complete Structure Solution, Refinement and Analysis Program, *J. Appl. Crystallogr.*, 2009, **42**, 339–341, DOI: 10.1107/S0021889808042726.

31 P. Giannozzi, S. Baroni, N. Bonini, M. Calandra, R. Car, C. Cavazzoni, D. Ceresoli, G. L. Chiarotti, M. Cococcioni, I. Dabo, A. Dal Corso, S. De Gironcoli, S. Fabris, G. Fratesi, R. Gebauer, U. Gerstmann, C. Gougoussis, A. Kokalj, M. Lazzeri, L. Martin-Samos, N. Marzari, F. Mauri, R. Mazzarello, S. Paolini, A. Pasquarello, L. Paulatto, C. Sbraccia, S. Scandolo, G. Sclauzero, A. P. Seitsonen, A. Smogunov, P. Umari and R. M. Wentzcovitch, QUANTUM ESPRESSO: A Modular and Open-Source Software Project for Quantum Simulations of Materials, *J. Phys.: Condens. Matter*, 2009, **21**, 395502, DOI: 10.1088/0953-8984/21/39/395502.

32 P. Giannozzi, O. Andreussi, T. Brumme, O. Bunau, M. B. Nardelli, M. Calandra, *et al.*, Advanced Capabilities for Materials Modelling with Quantum ESPRESSO, *J. Phys.: Condens. Matter*, 2017, **29**, 465901.

33 Z. Wang, X. H. Lv, Y. L. Liu, Y. Lu, H. P. Chen and J. Z. Ge, Prominent Dielectric Transitions in Layered Organic-Inorganic Hybrids: $(Isoamyl\text{-}Ammonium)_2CdX_4$ (X = Cl and Br), *Inorg. Chem. Front.*, 2017, **4**, 1330–1336, DOI: 10.1039/c7qi00270j.

34 Z. Wang, Y. Lu, H. P. Chen and J. Z. Ge, Controllable Structures Designed with Multiple-Dielectric Responses in Hybrid Perovskite-Type Molecular Crystals, *Inorg. Chem.*, 2017, **56**, 7058–7064, DOI: 10.1021/acs.inorgchem.7b00662.

35 M. Cannas, G. Carta, A. Cristini and G. Marongiu, Three-Co-Ordinate Thiocyanate in Cadmium Dithiocyanate, *J. Chem. Soc., Dalton Trans.*, 1976, 300–301, DOI: 10.1039/dt9760000300.

36 R. Jabbar and S. Kamoun, Synthesis, Molecular Structure and Theoretical Investigation of Optical and Electronic Properties of New Crystalline Polymer: $[(C_6H_5NH_3)_2Cd(SCN)_2Cl_2]N$, *J. Inorg. Organomet. Polym. Mater.*, 2020, **30**, 649–657, DOI: 10.1007/s10904-019-01321-x.

37 D. X. Liu, K. P. Xie, W. X. Zhang, M. H. Zeng and X. M. Chen, Structural Insights into a New Family of Three-Dimensional Thiocyanate-Bridged Molecular Double Perovskites, *CrystEngComm*, 2021, **23**, 2208–2214, DOI: 10.1039/d1ce00147g.

38 M. J. Cliffe, E. N. Keyzer, M. T. Dunstan, S. Ahmad, M. F. L. De Volder, F. Deschler, A. J. Morris and C. P. Grey, Strongly Coloured Thiocyanate Frameworks with Perovskite-Analogue Structures, *Chem. Sci.*, 2019, **10**, 793–801, DOI: 10.1039/c8sc04082f.

39 C. D. Oberle, D. G. Bequette, T. K. Brewer, T. R. R. Terry and A. M. Beatty, π-Choreography in Aromatic Ammonium Formate Solids, *CrystEngComm*, 2018, **20**, 1899–1907, DOI: 10.1039/c8ce00198g.

40 I. Hideta, V. G. Krishnan, S. Dou, H. Paulus and W. Alarich, Bromine NQR and Crystal Structures of Tetraanilinium Decabromotricadmate and 4-Methylpyridinium Tribromocadmate, *Z. Naturforsch., A:Phys. Sci.*, 1994, **49**, 213–222, DOI: 10.1515/zna-1994-1-233.

41 K. Saidi, S. Kamoun, H. F. Ayedi and M. Gargouri, Crystal Structure, NMR Study, Dc-Conductivity and Dielectric Relaxation Studies of a New Compound $[C_2H_{10}N_2]Cd(SCN)_2Cl_2$, *EPJ Web Conf.*, 2012, **29**, 1–11, DOI: 10.1051/epjconf/20122900031.

42 G. Tang, C. Yang, A. Stroppa, D. Fang and J. Hong, Revealing the Role of Thiocyanate Anion in Layered Hybrid Halide Perovskite $(CH_3NH_3)_2Pb(SCN)_2I_2$, *J. Chem. Phys.*, 2017, **146**, 224702, DOI: 10.1063/1.4984615.

43 (*a*) CCDC 2454582: Experimental Crystal Structure Determination, 2026, DOI: 10.5517/ccdc.csd.cc2nd62c; (*b*) CCDC 2454583: Experimental Crystal Structure Determination, 2026, DOI: 10.5517/ccdc.csd.cc2nd63d; (*c*) CCDC 2454584: Experimental Crystal Structure Determination, 2026, DOI: 10.5517/ccdc.csd.cc2nd64f; (*d*) CCDC 2454585: Experimental Crystal Structure Determination, 2026, DOI: 10.5517/ccdc.csd.cc2nd65g; (*e*) CCDC 2454586: Experimental Crystal Structure Determination, 2026, DOI: 10.5517/ccdc.csd.cc2nd66h; (*f*) CCDC 2454587: Experimental Crystal Structure Determination, 2026, DOI: 10.5517/ccdc.csd.cc2nd67j; (*g*) CCDC 2454588: Experimental Crystal Structure Determination, 2026, DOI: 10.5517/ccdc.csd.cc2nd68k.